

Neutrino induced charged-current coherent ρ production

X. C. Tian

Department of Physics and Astronomy, University of South Carolina, Columbia, SC, 29208, U.S.A.

E-mail: tianx@mailbox.sc.edu

Abstract. We present the latest results of coherent ρ (Coh ρ) production using the large data set collected by the NOMAD detector in which the momenta, charges, and photons are precisely measured. We discuss the application of using Coh ρ process to constrain the neutrino flux with the proposed Long-Baseline Neutrino Experiment Near Detector, the high resolution Straw Tube Tracker.

1. Introduction

With the discovery of non-zero θ_{13} by the reactor and accelerator neutrino experiments [1, 2] the focus has been shifted to the determination of neutrino mass hierarchy and the measurement of the leptonic CP violation phase, which may hold the key to the matter-antimatter asymmetry in the universe. To correctly interpret the oscillation data one needs to understand the neutrino-nucleon (nucleus) interaction thoroughly. The low momentum (Q^2) transfer, high energy (ν) transfer interactions of neutrino induced coherent ρ meson production allows us to study the basic properties of the weak current: the Conservation of the Vector Current hypothesis (CVC) [3, 4].

Based on the vector-dominance model [5], the differential cross section can be derived as [6]:

$$\frac{d^3\sigma(\nu_\mu\mathcal{A} \rightarrow \mu^-\rho^+\mathcal{A})}{dQ^2 d\nu dt} = \frac{G_F^2}{4\pi^2} \frac{f_\rho^2}{1-\epsilon} \frac{|q|}{E_\nu^2} \left[\frac{Q}{Q^2 + m_\rho^2} \right]^2 (1 + \epsilon R) \left[\frac{d\sigma^T(\rho^+\mathcal{A} \rightarrow \rho^+\mathcal{A})}{dt} \right], \quad (1)$$

where G_F is the weak coupling constant, $Q^2 = -q^2 = -(k - k')^2$, $t = (p - p')^2$, $\nu = E_\nu - E_\mu$, $x = Q^2/2M\nu$, $y = \nu/E_\nu$. f_ρ is related to the ρ form-factor, the polarization parameter $\epsilon = \frac{4E_\nu E_\mu - Q^2}{4E_\nu E_\mu + Q^2 + 2\nu^2}$, and $R = \frac{d\sigma^L/dt}{d\sigma^T/dt}$ with σ^L and σ^T as the longitudinal and transverse ρ -nucleus cross sections. The ρ form factor, f_ρ , is related to the corresponding factor in charged-lepton scattering, $f_{\rho^\pm} = f_{\rho^0}^\gamma \sqrt{2} \cos\theta_C$, where θ_C is the Cabibbo angle and $f_{\rho^0}^\gamma = m_\rho^2/\gamma_\rho$ is the coupling of ρ^0 to photon ($\gamma_\rho^2/4\pi = 2.4 \pm 0.1$).

Following the Rein-Sehgal model of meson-nucleus absorption [7],

$$\frac{d\sigma^T(\rho^+\mathcal{A} \rightarrow \rho^+\mathcal{A})}{dt} = \frac{\mathcal{A}^2}{16\pi} \sigma^2(\text{hn}) \exp(-b|t|) F_{\text{abs}}, \quad (2)$$

where $\sigma(\text{hn})$ is the ‘‘hadron-nucleon’’ cross-section with the energy of the hadron $\simeq \nu$, $b = R^2/3$ such that $R = R_0\mathcal{A}^{1/3}$, with $R_0 = 1.12$ fm and the absorption factor $F_{\text{abs}} = 0.47 \pm 0.03$.

2. The NOMAD Experiment

The NOMAD experiment is a short baseline neutrino experiment designed to search for $\nu_\mu \rightarrow \nu_\tau$ oscillations using the CERN Super Proton Synchrotron (SPS) wideband neutrino beam [8]. The 450 GeV protons from the SPS impinge on a beryllium target producing secondary mesons (K , π and K_L^0) which will produce neutrinos. The neutrino events dominated by ν_μ ($\nu_\mu : \bar{\nu}_\mu : \nu_e : \bar{\nu}_e = 1.00 : 0.025 : 0.015 : 0.0015$) have a mean energy of ~ 24 GeV spanning the region of $\mathcal{O}(1) \leq E_\nu \leq 300$ GeV. The NOMAD detector consists of several sub-detectors. 132 planes of 3×3 m² drift chambers (DC) with an average density similar to that of liquid hydrogen (0.1 g/cm³) serve as the active target. The fiducial mass of the DC is 2.7 tons with an effective atomic number, $A = 12.8$, similar to carbon. The DC provides excellent momentum resolution, $\sigma_p/p = 0.05/\sqrt{L(\text{m})} + 0.008p(\text{GeV})/\sqrt{L(\text{m})^5}$. The DC is followed by nine modules of transition radiation detectors (TRD), a pre-shower (PRS) and a lead-glass electromagnetic calorimeter (ECAL). The TRD, PRS, and ECAL sub-detectors provide a high-resolution efficiency and purity ($\geq 90\%$) of electron detection. A dipole magnet provides a 0.4 T magnetic field orthogonal to the neutrino beam direction that surrounds the DC, TRD, and PRS/ECAL. The magnet is followed by hadron calorimeter (HCAL) and two muon-stations comprising large area drift chambers separated by an iron filter placed at 8- and 13- λ 's downstream of the ECAL, and the muon-stations provide a clean identification of the muons.

The data used in this analysis were collected from 1995 to 1998 with 5.1×10^6 protons on target in neutrino mode, which corresponds to 1.4×10^6 ν_μ -CC interactions in the drift chamber. The Monte Carlo simulation of the coherent diffractive ρ process was done based on the diffraction model [5, 6, 9]. The details of data and MC have been described elsewhere [10].

3. Event Selection and Reconstruction

The $\nu_\mu + \mathcal{N} \rightarrow \mu^- \mathcal{N} \rho^+$ followed by $\rho^+ \rightarrow \pi^+ \pi^0$ has two tracks (μ^- and π^+) originating from the reconstructed primary vertex. The π^0 promptly decays into two photons. The two photons either both convert in the drift chamber (2 V_0 s event), or one of the photons converts in the drift chamber and the other is measured in the electromagnetic calorimeter (1 V_0 1 cluster event), or both photons are measured in the ECAL (2 cluster event).

The two-track Monte Carlo events with an identified muon within the fiducial volume that pass the following preselection cuts are used to build a likelihood ratio to separate the signal from background. These preselection cuts are 1) the opening angle between μ^- and π^+ (θ_{μ^-, π^+}) is less than 0.5 rad, 2) the π^+ energy (E_{π^+}) is greater than 1 GeV, 3) the missing transverse momentum (p_m^T) is less than 0.5 GeV, and 4) the event should have either 2 V_0 s, 1 V_0 plus 1 cluster, or 2 clusters.

4. The Results

The Bjorken variables x , y and \mathcal{Z}_{π^+} defined as $E_{\pi^+} \times (1 - \cos \theta_{\pi^+})$ are used to construct the likelihood $\mathcal{L} = \ln \frac{P(l|\text{Coh}\rho^+)}{P(l|\text{BKG})}$ to select the signal events. Figure 1 shows the likelihood distribution, and the signal region is defined as $\mathcal{L} > 1.8$. An independent analysis using the neural network (NN) under the ROOT framework [11] gives very consistent results. Table 1 shows the numbers (background, raw data, efficiency and fully corrected Coh ρ^+ signal events) in the signal region obtained from both likelihood and NN analysis. The total systematic uncertainty is $\pm 3.9\%$ which comes from 1) $\pm 1.6\%$ background normalization error dominated by charged-current Deep Inelastic events which is obtained by using the control region in likelihood or NN, 2) $\pm 2.5\%$ absolute normalization error which is from the inclusive charged current cross section measurement [10], and 3) $\pm 2.5\%$ signal efficiency related error which is found by varying the likelihood or NN cut, difference between likelihood and NN, and mock data study.

Using the measured inclusive ν_μ -CC cross-section from [10] as a function of E_ν , the absolute cross-section of Coh ρ^+ production for $A = 12.8$ at the average energy of the neutrino flux

$E_\nu = 24.8$ GeV is determined to be:

$$\sigma(\nu_\mu + \mathcal{N} \rightarrow \mu^- \mathcal{N} \rho^+) = [67.1 \pm 4.8 (\text{stat}) \pm 2.6 (\text{syst})] \times 10^{-40} \text{ cm}^2/\text{nucleus}, \quad (3)$$

which is consistent with the prediction and previous measurements but with much better precision. Table 2 is a compilation of the measurements up to today. Figure 2 shows the $\text{Coh}\rho^+$ cross section as a function of incoming neutrino energy with other measurements and predictions based on different models [17]. NOMAD data agree with the CVC and VDM based model prediction fairly well. The measurement favors the model with $R = 0$, *i.e.* there is little longitudinal contribution in $\text{Coh}\rho^+$ production.

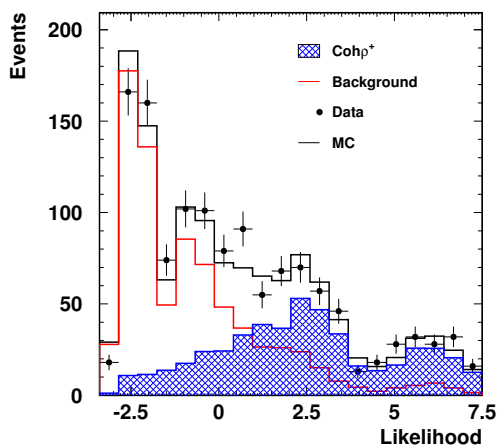


Figure 1. The likelihood \mathcal{L} distribution for data (points with error bars) and MC.

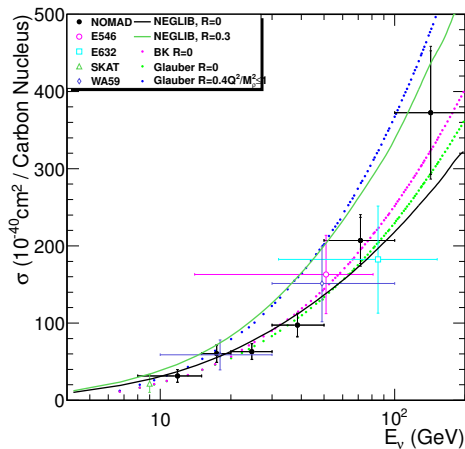


Figure 2. The $\text{Coh}\rho^+$ cross section as a function of incoming neutrino energy with different measurements and predictions.

Table 1. The results are obtained based on two independent analysis algorithms.

Algorithm	Background	Data	Efficiency	$\text{Coh}\rho^+$ Signal
Likelihood	86.1	363	0.064	4318.8 ± 307.4
NN	76.1	356	0.065	4332.0 ± 319.4

5. Discussion

The precision determination of relative and absolute neutrino flux is essential to any neutrino oscillation and cross section measurements, especially in the precision era. The primary goal of the Long-Baseline Neutrino Experiment (LBNE) is to determine the neutrino mass hierarchy and to observe CP violation. The proposed high-resolution LBNE Near Detector [18, 19] (Figure 3) could make measurements that would significantly enhance LBNE's overall sensitivity. Measurements required to achieve LBNE's primary objectives include the relative abundance and energy spectra of all four neutrino species, ν_μ , $\bar{\nu}_\mu$, ν_e , $\bar{\nu}_e$; neutrino and antineutrino cross-sections. Besides the insight into the weak current by studying the $\text{Coh}\rho^+$ interactions, one

Table 2. A compilation of the charged-current coherent ρ measurements.

Experiment	$\nu/\bar{\nu}$	Channel	Target	$\langle E_\nu \rangle$ (GeV)	σ (10^{-40} cm ² /nucleus)
E546 [12]	ν	ρ^+	Neon (A=20)	51	189.7±59
BEBC WA59 [13, 14]	$\bar{\nu}$	ρ^-	Neon (A=20)	18	73±23
E632 [15]	$\nu + \bar{\nu}$	ρ^\pm	Neon (A=20)	86	210±80
SKAT [16]	ν	ρ^+	Freon (A=30)	10	29±16
NOMAD (This Exp.)	ν	ρ^+	Carbon (A=12.8)	24.8	67.1±5.4

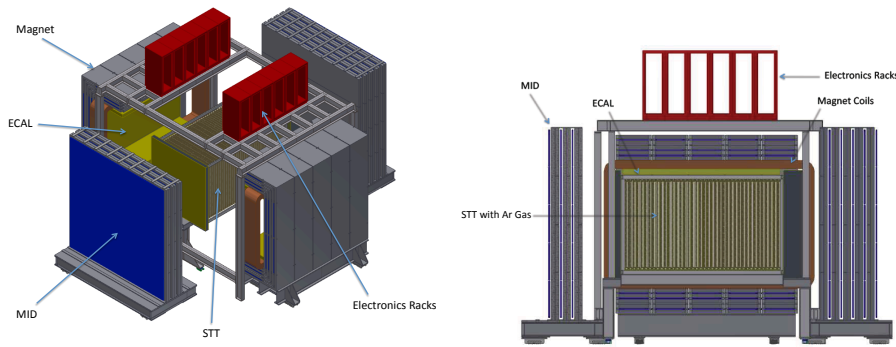


Figure 3. The proposed LBNE Near Detector - high resolution straw tube tracker.

can use this process to measure the absolute neutrino flux with high precision under the scope of CVC. The LBNE Near Detector will have a much higher resolution and statistics, which permits us to better understand the space-time structure of the weak current, and to advance our understanding of the neutrino flux.

References

- [1] An F P *et al.* 2012 *Phys. Rev. Lett.* **108** 171803 (Preprint: hep-ex/1203.1669)
- [2] Ahn J K *et al.* 2012 *Phys. Rev. Lett.* **108** 191802 (Preprint: hep-ex/1204.0626)
- [3] Feynman R P and Gell-Mann M 1958 *Phys. Rev.* **109** 193
- [4] Adler S L 1964 *Phys. Rev.* **135** B193
- [5] Piketty C A and Stodolsky L 1970 *Nucl. Phys. B* **15** 571
- [6] Kopeliovich B Z and Marage P 1993 *Int. J. Mod. Phys. A* **08**, 1512
- [7] Rein D and Sehgal L M 1983 *Nucl. Phys.* **223** 29
- [8] Altegoer J *et al.* 1998 *Nucl. Instr. and Meth. A* **404** 96
- [9] Hyett N M 1998 Coherent Diffractive ρ Production by Neutrinos in NOMAD Ph.D. Thesis
- [10] Wu Q *et al.* 2008 *Phys. Lett. B* **660** 19 (Preprint: hep-ex/0711.1183)
- [11] <http://root.cern.ch/drupal>
- [12] Ballagh H C *et al.* 1988 *Phys. Rev. D* **37** 1744
- [13] Marage P *et al.* 1984 *Phys. Lett. B* **140** 137
- [14] Marage P *et al.* 1987 *Z. Phys C* **35** 275
- [15] Willocq S *et al.* 1993 *Phys. Rev. D* **47** 2661
- [16] Agababyan N M *et al.* 2011 *Phys. Atom. Nucl.* **74** 221
- [17] The Glauber and BK predictions are from the digitization of Ref. [15], then scaled to the NOMAD target
- [18] Mishra S R, Petti R and Rosenfeld C 2008 Preprint: hep-ex/0812.4527
- [19] Mishra S R 2010 *Prog. Part. Nucl. Phys.* **64** 202